

Microthrusters in Silicon for Aerospace Application

Lamedica Giulio, Balucani Marco and Ferrari Aldo,
Electronic Department, University of Rome "La Sapienza" &
Tromboni Pier Domenico and Marchetti Mario,
Aerospace Department, University of Rome "La Sapienza"

ABSTRACT

This paper reviews the results of the thermal and static analysis of Small Motor AerospaCe TecnoLogy (SMART) propulsion system, constituted of a microthrusters array realised by MEMS technology on silicon wafers. This system has been studied using FEM (NASTRAN) and the results have been verified by the electro-thermic analogy and the FDM method, using, respectively, SPICE and MATLAB codes. The simulation results demonstrated the feasibility of SMART systems for aerospace applications as attitude control and deorbiting missions for small satellite station-keeping. A theoretical impulse of 20 mNs has been calculated for the SMART system.

NOMENCLATURE

R_{irr}	Radiative resistance (Ω)
R	Electric resistance (Ω)
C	Electric capacitor (Farad)
A_t	Total radial area (m^2)
h_{irr}	Radiative coefficient ($W/m^2 K$)
σ_0	Coblenz constant ($5.7 \cdot 10^{-8} W/m^2 K^4$)
T	Temperature ($^{\circ}C$)
k_{si}	Thermal conductivity of silicon (W/mK)
k	Thermal conductivity (W/mK)
s	Wall thickness (m)
A	Total normal surface (m^2)
ρ	Density (Kg/m^3)
t_c	Combustion time (s)
Q_c	Heat of combustion of the GAP (J)
c_p	Specific heat at constant pressure ($J/Kg K$)
A_{tot}	Total lateral surface of the chamber (m^2)

Authors' Current Addresses:

L. Giulio, B. Marco and F. Aldo, INFN-Unit E6, Electronic Department, Engineering Faculty, University of Rome "La Sapienza," Via Eudossiana, 18-00184 Roma, Italy; T.P. Domenico and M. Mario, INFN-Unit E6, Aerospace Department, Engineering Faculty, University of Rome "La Sapienza," via Eudossiana, 18-00184 Roma, Italy.

Based on a presentation at Battery 2002.

0885/8985/02/ \$17.00 © 2002 IEEE

INTRODUCTION

The new microspacecraft concepts push the micropropulsion system to decrease its mass and dimension, and, in this direction, move aerospace research activities.

Arrays of one-shot microthrusters in a three-layer sandwich configuration, electrically ignited, have been fabricated by Aerospace, TRW, Inc., and the Californian Institute of Technology, in Pasadena [1]. The power necessary to carry the resistance to the temperature of ignition of the propellant has been estimated to be 70 mW [2]. The bottom wafer is placed on the outer surface of the picosat. Estimates that the necessary impulse can be overcome providing $\cong 1\mu NS$ to $1 \cong mNs$ every 10 to 100 seconds throughout each satellite's mission [3]. The test of the three-layer system, using lead styphnate as propellant, have produced a specific impulse of 0.1 mNs but have shown a very low efficiency, only of the 10% [4]. The LAAS-CNRS has proposed a millimetre-scale microthruster operating at subsonic speed and delivering a low thrust level for a few hundreds of milliseconds [5].

The SMART project, born from the collaboration between the Aerospace Department and the Department of Electronics of the Engineering Faculty of the University of Rome "La Sapienza" and funded by the Italian Space Agency (ASI), proposes a new microthruster system for small satellites with a high propulsion efficiency. The SMART project using Micro Electro-Mechanical Systems (MEMS) technology realises different sized combustion chambers on the same silicon wafer, permitting the thrust modulation. Furthermore, the use of MEMS technologies predicts low cost in comparison with the technologies normally used for the realization of propulsion systems.

CONFIGURATION

The fundamental concept on which the SMART system is based consists of obtaining microthruster array starting from silicon wafers {100} utilizing its surface, instead of thickness.

In this way it is possible to obtain the high chamber volume ($50 mm^3$) able to contain a high quantity of the propellant (0.1 g). The thruster is realised etching a masked silicon wafer with KOH or TMAH [6]. This process allows us to obtain different

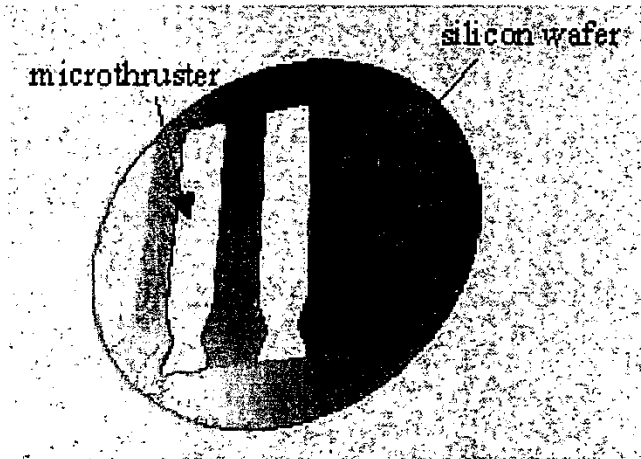


Fig. 1. Views of the microthrusters in the silicon wafer (100) (diameter 4 inch, thickness 1 mm)

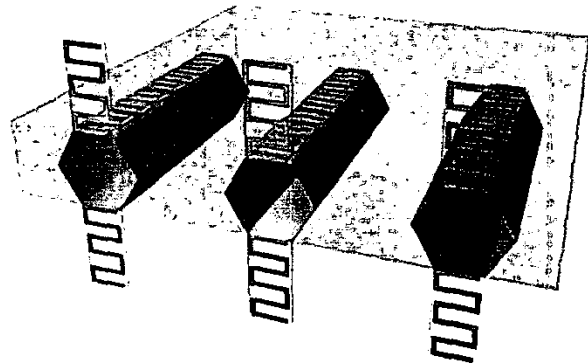


Fig. 3. View of microthruster row, particular of copper wire able to the ignition of the propellant



Fig. 2.

Fig. 2. Microthrusters array; particular of the copper wire necessary to the dissipation through radiation

shapes both for the combustion chamber and the nozzle, whose shape and dimensions can be varied in function of the operating conditions to which the system is dedicated. The combustion chamber and the nozzle are realised as shown in Figure 1. In order to obtain single rows of the microthrusters array, the two wafers are processed in the same way and bonded together by the Silicon Direct Bonding process (SDB), which allows us to form covalent bounds, thanks to the contemporaneous use of pressure (atmospheric pressure or vacuum) and high temperature

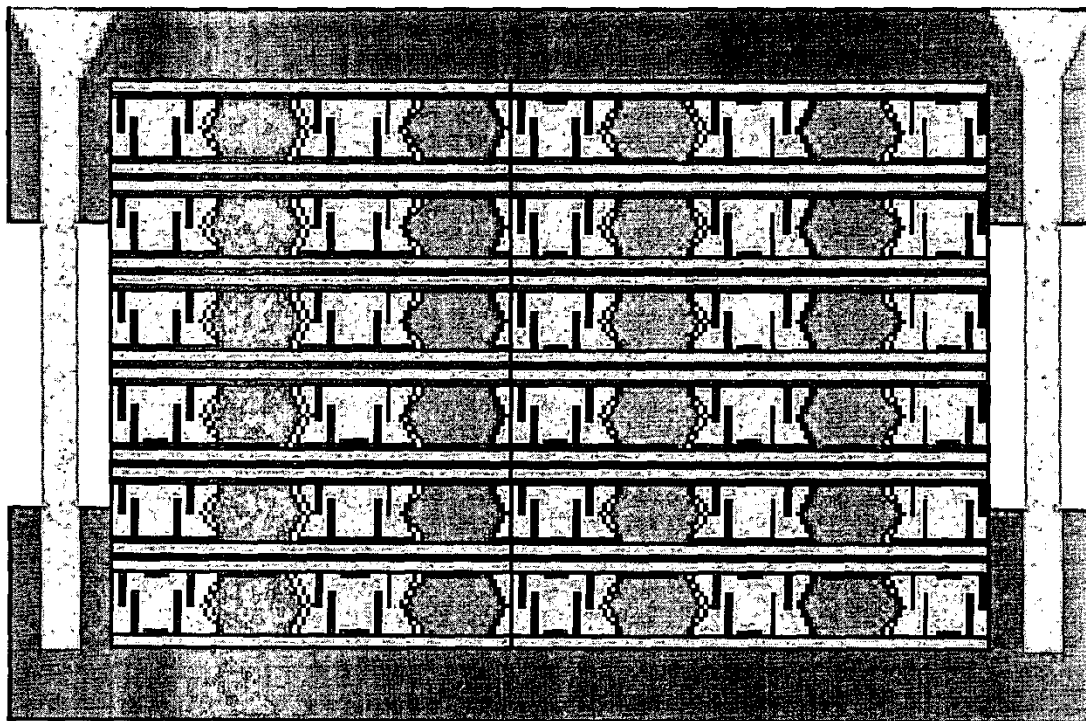


Fig. 4. Model of 5 × 5 microthrusters array

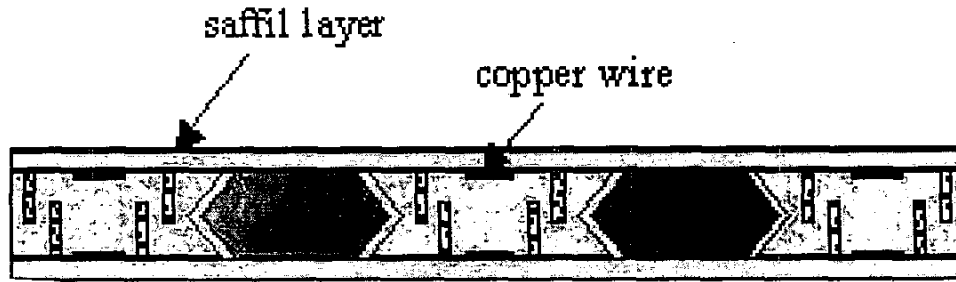


Fig. 5. Row of array; the particular of the copper wire and saffil layer can be seen

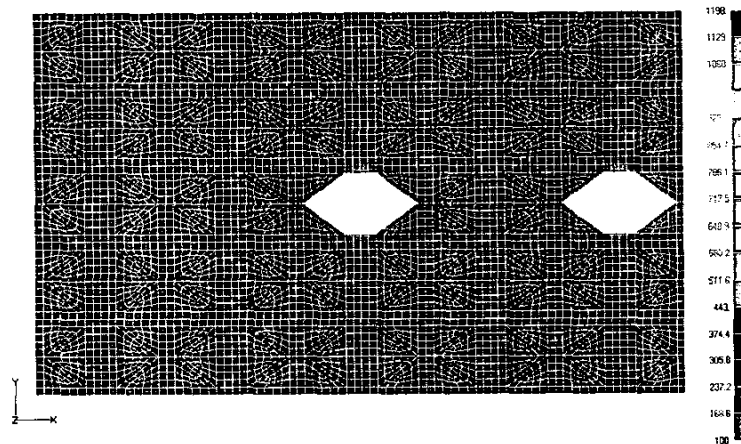


Fig. 6. Result of NASTRAN simulation for the first configuration; it shows the distribution of the temperatures to the instant $t = 50$ ms, when two chambers are ignited

(1000 °C) [7]. Using 4 inch wafers and fixing the height of the combustion chamber equal to 5 cm and the distance between the chamber equal to 0.5 mm, it is possible to obtain 18 microthruster cells for each wafer. The frontal section of the nozzle considered is hexagonal-shaped, 1 mm height and 4.74 mm wide, as shown in Figure 2. This shape is due to the etching angle, technologically imposed as 54.45° for silicon wafer {100} [8]. A diaphragm of silicon nitride (Si_3N_4) preserves the nozzle from the effects of the external environment. The diaphragm must be weak enough to be broken by the pressure of the gases. A double layer of $\text{ZrO}_2/\text{Y}_2\text{O}_3$, 1 micron thick, and a layer of SiO_2 , 50 1 μm thick, have been deposited by the Chemical Vapour Deposition (CVD) process on the silicon walls of each chamber. These layers have been introduced to limit the combustion heat propagation. The ignition of the propellant is obtained by electrical thin film resistances, as shown in Figure 3 which are deposited by CVD process, along the walls of the combustion chamber. The used propellant is Glycidyle Azide Polymer (GAP), due to its properties that make it particularly suitable for propulsive purposes:

- Characteristic of deflagration (1.3c UN shipping classification);
- Low auto-ignition temperature (216° C);

- Low flame-temperature.

The final structure of the microthrusters array, shown in Figure 4, is obtained from the stacking of a number of rows, such as a microthruster, enough to provide the required thrust.

THERMAL ANALYSIS

The thermal analysis was carried out to evaluate the limits of the proposed configuration. The most critical hypothesis of explosion within a closed cavity has been considered. This condition is equivalent to consider the diaphragm, which closes the nozzle and separates it from the external environment, infinitely rigid. The simulation has been carried out to verify that the thermomechanical effect produced by the explosion does not cause the spontaneous ignition of propellant contained in adjacent chambers. This case is critical for configuration due to the small distance between each combustion chamber. In this configuration, each row has been isolated by a saffil layer and the heat generated by combustion is conveyed toward the lateral surfaces of the system by copper wires disposed parallelly to the chamber axis, as shown in the cross-section of a microthruster row (Figure 5).

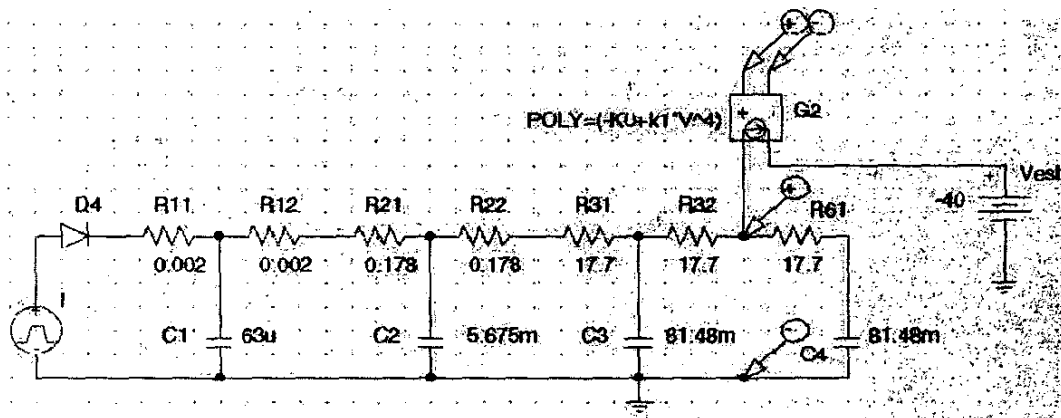


Fig. 7. Electric model utilised in the electro-thermic analogy method

According to this configuration, the case in which a chamber undergoes to the contemporaneous thermal effects of the two contiguous chambers has been simulated using a finite element method (FEM). An unsteady thermal analysis on a bi-dimensional model of the system has been made using NASTRAN as FEM code. The following boundary conditions have been imposed in the simulation:

- a body temperature (100° C) due to direct radiation and Albedo effects;
- a starting temperature of the walls chamber equal to the ignition temperature of the GAP (216° C);
- an irradiation condition along the external walls of the array; and
- a thermal flow entering in the walls of the chambers in which the combustion happens.

The thermal flow has been estimated, in function of the properties of the propellant and its burning rate, through expression relating combustion heat of the GAP, total lateral surface of the chamber, and combustion time.

The burning rate has been estimated by means of the law of Vieille. Because of the difference between the thickness of the insulating layers (ZrO_2/Y_2O_3 and SiO_2) and silicon, the FEM model has been designed without insulating layers. In order to consider the thermal effects of the insulating layers, the value of the outflow from the insulating layers has been utilised as input in the FEM model. As such, the heat portion dissipated by the ZrO_2/Y_2O_3 and SiO_2 layers has been considered.

Figure 6 shows the situation after 50 ms from the ignition of the propellant. The maximum temperature (236.77° C), higher than the auto ignition of the GAP is reached on the wall of the neighbour off chamber. The results obtained by the FEM simulation have been verified by the electro-thermic analogy method. An equivalent electric system has been designed as shown in Figure 7. Each layer (ZrO_2/Y_2O_3 , SiO_2 , Si, etc.) of the wall between two adjacent chambers, has been considered as a plane wall and modelled with two electrical resistances in

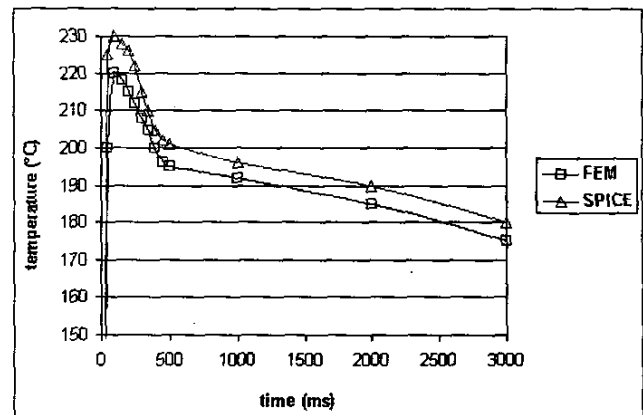


Fig. 8. Results of NASTRAN and SPICE simulations; the distribution of nodal temperatures vs. time is seen

parallel with a capacitor. For plane walls, the resistances R and capacitors C are related by the thickness of the layer, the thermal conductivity of the layer, the total normal surface, and the density of the wall.

The combustion effects have been represented using a polynomial voltage controlled current source (VCCS) generator. The amount of charge released by the VCCS in a period equal to the combustion time, is the same as the amount of the heat generated by the combustion; subsequently, the voltage generator acts as a short-circuit. A diode valve has been introduced after the generator to avoid the discharge of the capacitors in the short-circuit configuration. The radiation effects have been represented as a voltage generator, current controlled, with relationships between Coblenz constant, total radiative surface, body temperature, and external temperature.

The results of the SPICE simulation are in agreement with the results of FEM simulation, unless a scaling temporal factor, due to the electric configuration as shown in Figure 8. Both simulations revealed that such kind of system configuration is not utilizable because the wall of the off chamber is higher than the propellant ignition temperature.

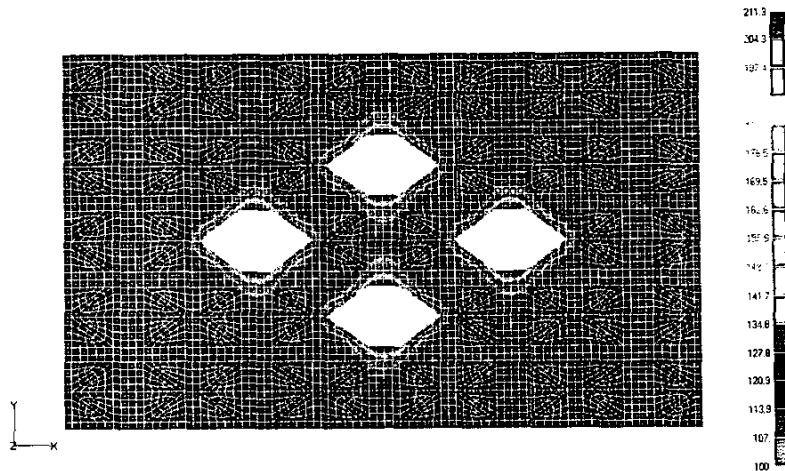


Fig. 9. Result of NASTRAN simulation for the second configuration studied; it shows the distribution of temperatures to the instant $t = 500$ ms, after the four chamber simultaneous ignition

A new configuration without saffil layers has been studied and analysed. The insulated layers have been removed to benefit of the high conductivity of silicon ($k_{si} = 141.2$ W/m K). For this configuration, the thermal effects of the four chambers around the off chamber have been considered. The more critical situation ($t = 500$ ms) is shown in Figure 9. The maximum temperature value is 211.3°C and has been reached on the wall of the on chamber. In spite of the simultaneous ignition of four microthrusters, the off chamber reaches, at this time, a maximum temperature of about 140°C , that is less than the propellant ignition temperature. This behaviour is due to the greatest silicon region interested by the heat exchange; the flux lines are almost concentric circumferences, whose radius increases with time. Also, in this case, the NASTRAN results have been verified. To this purpose, a MATLAB program, based on a monodimensional discrete Fourier equation, has been implemented by an implicit upwind finite differences method (FDM) with an expression where T , the nodal temperature, N , is the node number and α , β are coefficients related to the properties of the $\text{ZrO}_2/\text{Y}_2\text{O}_3$, SiO_2 , Si layers. The region between two chambers have been divided in forty-nine intervals introducing fifty nodes ($N = 50$). The following boundary conditions have been imposed:

- a thermal flow (q), entering in the wall of the chamber on (first node), equal to the thermal flow has been precedently calculated, including the thermal exchange coefficient between the combustion gases and the wall of the on chamber;
- an adiabatic condition ($q = 0$) on the wall of the off chamber (last node).

The nodal temperature, obtained until 250 ms after the ignition of the propellant, are in agreement with the results

obtained from the NASTRAN simulations at the 500 ms. The disagreement of the wall temperature value in correspondence of the on chamber is due to the monodimensional model utilized in the FDM model and to the imposed adiabatic condition on the last node of the model.

STATIC ANALYSIS

A static analysis has been conducted to verify that the pressure loads, produced by the combustion, do not shatter the chamber walls. Only half of the chamber has been considered due to the axial symmetry of the thruster. The Young modulus of the silicon has been evaluated at the highest temperature value provided by thermal analysis [9]. The following constraint conditions have been imposed on a single thruster:

- fixed at the bottom of the combustion chamber;
- free at the far end of the nozzle;
- the symmetric constraint along the walls in touch with adjacent thrusters.

The chamber geometry predicts that the region more stressed is the wafer bounding surface near the fixed tip.

A 60 MPa pressure estimated as the maximum allowable load was temporarily created on the inner wall of the solid NASTRAN model (brick elements), though usually the combustion pressure is about 10-15 MPa in service conditions. Figure 10 confirms that the bonding surface is the more stressed region and the value of the y normal stress is very close to the debonding limit of the silicon wafers [10]. The stress values, reported in the Figure 9, are in N/mm^2 , with negative values depicting compressive stress and positive values depicting tensile stress. In this the total translation is equal to $3.5 \mu\text{m}$. A specific theoretical impulse of I_s 20 mNs has been calculated under the following hypothesis:

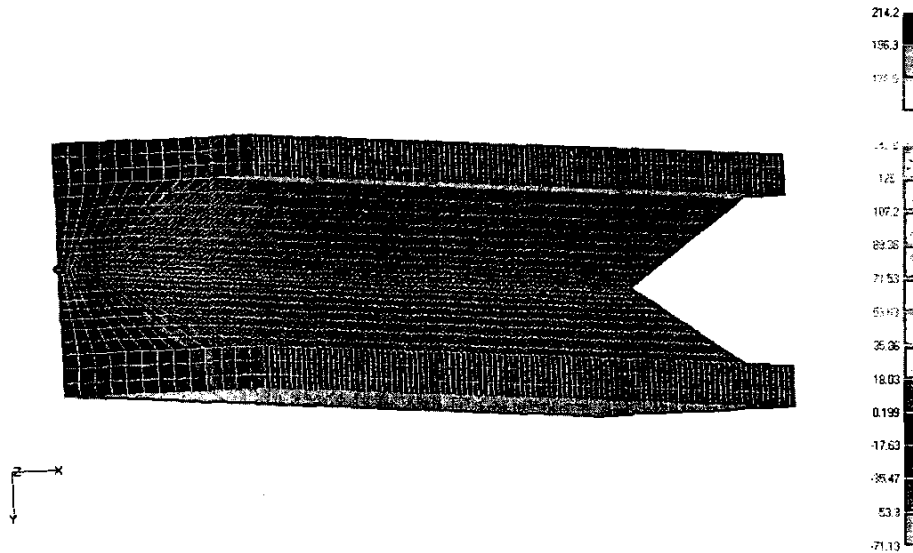


Fig. 10. Result of static analysis in the NASTRAN simulation; the distribution of the normal stress in the semichamber model can be seen

- propulsive efficiency of 60% (generally the efficiency is closely 50-80%);
- efflux velocity equal to 1/5 of combustion rate;
- mass of GAP equal to 20.45 mg.

CONCLUSION

In this paper a suitable configuration for the Small Motor Aerospace Technology (SMART) system has been identified. Thermal and static analyses have been performed to verify the performances of the system in operating conditions. The results obtained by FEM, FDM, and electro-thermic analogy are in agreement between them, demonstrating the consistency of the models used. For the identified configuration, a specific theoretical impulse of 20 mNs has been calculated. These data are going to be verified through the experimental set-up, which is being carried out currently.

ACKNOWLEDGMENT

SMART Project, funded by the Italian Space Agency, No. 6707 (01) SME G & A Engineering (ITALY) for packaging and bonding.

REFERENCES

- [1] E. Choueri, J.B. Neidert, R.E. Black, III, K.J. Graham and R. Lucas, August 21-24, 2000, USU Conference on Small Satellites Paper: SSC00-X-2, Presented at the 14th AIAA/USU Small Satellite Conference, North Logan, UT.
- [2] C. Rossi, D. Esteve and C. Mingues, (1999), Pyrotechnic actuators: a new generation of Si integrated circuit, *Sensor and Actuators* 74 (1999) 211-214.
- [3] D.W. Youngner, S. Thai Lu, E. Choueri, J.B. Neidert, R.E. Black, K.J. Graham, D. Fahey, R. Lucas and X. Zhu, 2000, MEMS mega-pixel array for small satellite stationkeeping, 14th Annual/USU Conference on Small Satellites.
- [4] D.H. Lewis, Jr., S.W. Jansonb, R.B. Cohen and E.K. Antonsson, 2000, Digital micropropulsion, *Sensor and Actuators* 80, 143-154.
- [5] C. Rossi, M.D. Rouhani and D. Esteve, 5 November 1999, Prediction of the performance of a Si-micromachined microthruster by computing the subsonic gas flow inside the thruster.
- [6] M. Shikida, K. Sato and D. Uchikawa, (2000), Differences in anisotropic etching properties of KOH and TMAH solutions, *Sensor and Actuators* 80, 179-188.
- [7] A. Ploéul and G. Kraéuter, 12 October 1998, Wafer direct bonding: tailoring adhesion between brittle materials, Max Planck Institute fu er Mikrostrukturphysik, Weinberg 2, D-06120, Halle (Saale), Germany.
- [8] I. Zobel and I. Barycka, (1998), Silicon anisotropic etching in alkaline solutions 1. The geometric description of figures developed under etching Si (100) in various solutions, *Sensor and Actuators A* 70, 250-259.
- [9] Graded final thesis dissertation, P.D. Tromboni, 13 July 2001, Studio di sistemi innovative per la stabilizzazione di piattaforme spaziali, Chapter 3, pp.45-49, Rome.
- [10] A. Ploéul and G. Kraéuter, October 1998, Max-Planck-Institute fu Er Mikrostrukturphysik, Wafer direct bonding: tailoring adhesion between brittle materials, Weinberg 2, D-06120, Halle (Saale), Germany, Accepted October 12, 1998.